Realistic MHD simulations of the Evershed flow in a sunspot penumbra

By I. N. Kitiashvili, A. G. Kosovichev, A. A. Wray AND N. N. Mansour

1. Motivation and objective

In the spring of 1909 Evershed published a remarkable discovery of strong horizontal mass flows in sunspots penumbra, the outer part of sunspots characterized by filamentary magnetic field structures (Evershed 1909). The flows, with typical speed of $1-4$ km/s (Mach number $0.2-0.7$), start at the boundary between the umbra and penumbra and expand radially, accelerating with distance and suddenly stopping at the outer sunspot boundary. The Evershed effect may play significant role in the formation, stability, and dynamics of sunspots and is considered one of the fundamental process in solar physics. This phenomenon caused significant interest and detailed observational and theoretical investigations, but the understanding of the physical mechanism is still missing (a recent review is published by Tritschler 2009).

High-resolution observations from large ground-based telescopes and the Hinode space mission revealed a complicated filamentary structure of these flows (Rimmele 1994, 1995; Ichimoto *et al.* 2007a,b) and their non-stationary dynamics in the form of fast ($M \sim 1$) quasiperiodic flow patterns "Evershed clouds" (Shine *et al.* 1994; Rimmele 1994; Georgakilas & Christopoulou 2003; Cabrera Solana *et al.* 2007, 2008). In some cases, the flows show a large-scale coherent organization across several flow channels (Shine *et al.* 1994) and also a wave-like behavior (Rimmele 1994; Georgakilas & Christopoulou 2003).

Theories of the Evershed effect can be divided in two categories: as channel flows in magnetic flux tubes (Meyer & Schmidt 1968; Montesinos & Thomas 1997; Schlichenmaier *et al.* 1998) or as elongated magnetoconvective rolls (Danielson 1961; Hurlburt *et al.* 2000). Recent numerical simulations (Heinemann *et al.* 2007; Rempel *et al.* 2009) successfully modeled the filamentary magnetic structure of sunspot penumbra and horizontal outflows, thus providing a strong support for the magnetoconvective nature of the Evershed effect (Scharmer *et al.* 2008).

In this paper, we present a study of solar magnetoconvection in the presence of an inclined magnetic field, based on the realistic radiative MHD simulations, and link the Evershed effect to the phenomenon of traveling magnetoconvection waves. The convective waves is an interesting MHD phenomenon (Weiss 1991), which, in fact, has been previously suggested as a reason for the Evershed flows (Hurlburt *et al.* 2000), but the suggestion was not developed further. Our study provides a basis for explaining the Evershed effect as a result of traveling magnetoconvection waves in highly inclined magnetic field of sunspot penumbra. The phenomenon of traveling magnetoconvection waves is considered also in the dynamics of the Earth's core (Walker & Barenghi 1999; Zhang 1999),and may happen in various astrophysical objects, such as magnetic stars, accretion disks, compact objects and active galactic nuclei. Thus, detailed observational and theoretical studies of this phenomenon are of great interest.

2. Numerical simulations

We use a three-dimensional, non-linear radiative-magnetohydrodynamics code developed for simulating the upper solar convection zone and lower atmosphere (Jacoutot *et al.* 2008a,b). This code takes into account several physical phenomena: compressible fluid flow in a highly stratified medium, three-dimensional multi-group radiative energy transfer between the fluid elements, a real-gas equation of state, ionization and excitation of all abundant species, and magnetic effects. Because both the Reynolds number and magnetic Reynolds number are very high, an important feature of this code is implementation of various subgrid scale LES turbulence models. Here we adopted the most widely used Smagorinsky model (Smagorinsky 1963) in the compressible formulation (Moin *et al.* 1991; Germano *et al.* 1991). The turbulent electrical conductivity is calculated by using the extension of the Smagorinsky model to the MHD case (Theobald *et al.* 1994).

The governing equations are the grid-cell averaged conservations of mass (2.1), momentum (2.2), energy (2.3), and magnetic flux (2.4):

$$\frac{\partial \rho}{\partial t} + \left(\rho u_i\right)_{,i} = 0, \tag{2.1}$$

$$\frac{\partial \rho u_i}{\partial t} + \left(\rho u_i u_j + (P_{ij} + \rho \tau_{ij})\right)_{,j} = -\rho \phi_{,i}, \tag{2.2}$$

$$\frac{\partial E}{\partial t} + \left[E u_i + (P_{ij} + \rho \tau_{ij}) u_j - (\kappa + \kappa_T) T_{,i} + \left(\frac{c}{4\pi}\right)^2 \frac{1}{\sigma + \sigma_T} \left(B_{i,j} - B_{j,i}\right) B_j + F_i^{rad} \right]_{,i} = 0, \tag{2.3}$$

$$\frac{\partial B_i}{\partial t} + \left[u_j B_i - u_i B_j - \frac{c^2}{4\pi(\sigma + \sigma_T)} \left(B_{i,j} - B_{j,i}\right) \right]_{,j} = 0, \tag{2.4}$$

where ρ is the averaged mass density, u_i is the Favre-averaged velocity, B_i is the magnetic field, and E is the averaged total energy density $E = \frac{1}{2}\rho u_i u_i + \rho e + \rho \phi + \frac{1}{8\pi} B_i B_i$, where ϕ is the gravitational potential and e is the Favre-averaged internal energy density per unit mass. F_i^{rad} is the radiative flux, which is calculated by solving the radiative transfer equation, and P_{ij} is the averaged stress tensor $P_{ij} = \left(p + 2\mu u_{k,k}/3 + \frac{1}{8\pi} B_k B_k\right) \delta_{ij} - \mu \left(u_{i,j} + u_{j,i}\right) - \frac{1}{4\pi} B_i B_j$, where μ is the viscosity. The gas pressure p is a function of e and ρ through a tabulated equation of state (Rogers *et al.* 1996); τ_{ij} is the Reynolds stress, κ is the molecular thermal conductivity, κ_T is the turbulent thermal conductivity, σ is the molecular electrical conductivity, and σ_T is the turbulent electrical conductivity.

We simulate the upper layer of the convection zone, extending from 5 Mm below the visible surface to 0.5 Mm above the surface. The horizontal size varied from 6.4 Mm $\times$ 6.4 Mm to 25 Mm $\times$ 25 Mm. The computational grid step size varied from 25 to 100 km. The results were obtained using a 128^3 grid with the step size of 50 km. We have verified that the results do not change in computations with finer grids (except for the development of smaller scale turbulent motions).

The initial uniform magnetic field is imposed on a snapshot of the preexisting hydrodynamic convection (Jacoutot *et al.* 2008b). The initial field strength, B_0, varies from 0 to 2000 Gauss, and the inclination angle, α, varies from 0 to 90 degrees. The lateral boundary conditions are periodic, and the top and bottom boundary conditions maintain the total magnetic flux and the mean inclination. This formulation allowed us to carry out a series of controlled numerical experiments and investigate how the structure and dynamics of solar turbulent convection depended on the magnetic field properties in regimes

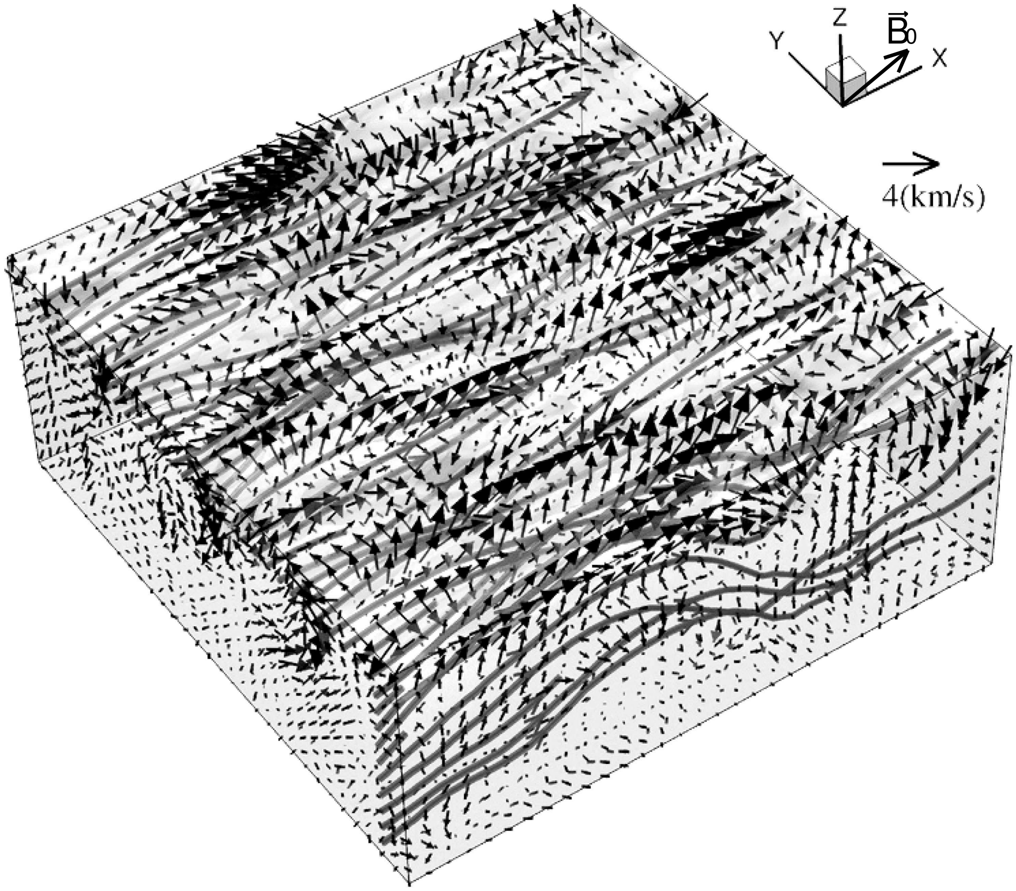

FIGURE 1. A snapshot of the three-dimensional simulations of subsurface solar convection in a region of an inclined magnetic field. The initial field strength, B_0, is 1000 G, the inclination angle, α, is 85 degrees with respect to the vertical. Grey curves show magnetic field lines; the arrows show the velocity field. The horizontal size of the box is 6.4 Mm, the depth is about 2.5 Mm.

close to the observed in sunspot penumbra, and elucidated the physical mechanism of the Evershed effect.

3. Results

Outside magnetic field regions the solar convection forms granular cells of a typical size of $1 - 2$ Mm and lifetime of about 10 min. In the presence of magnetic field the structure of convection strongly depend on the field strength and inclination (Fig. 1, 2). When the magnetic field is vertical the granules become smaller (Stein & Nordlund 2002), and their overturn time is shorter resulting in generation of high-frequency turbulence and acoustic waves ("halos") (Jacoutot *et al.* 2008b). In the presence of an inclined magnetic field, such as observed in sunspot penumbra, the granular cells becomes naturally elongated in the direction of the field because magnetic field restricts motions across the magnetic field lines. But the most interesting effect is that the inclined field changes the nature of solar convection. Instead of a stationary overturning convection pattern the simulation reveal

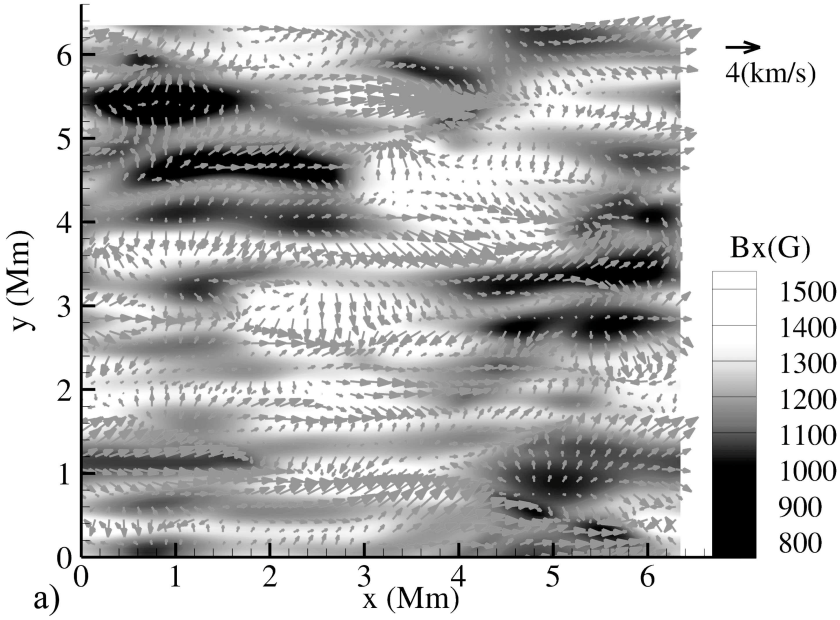

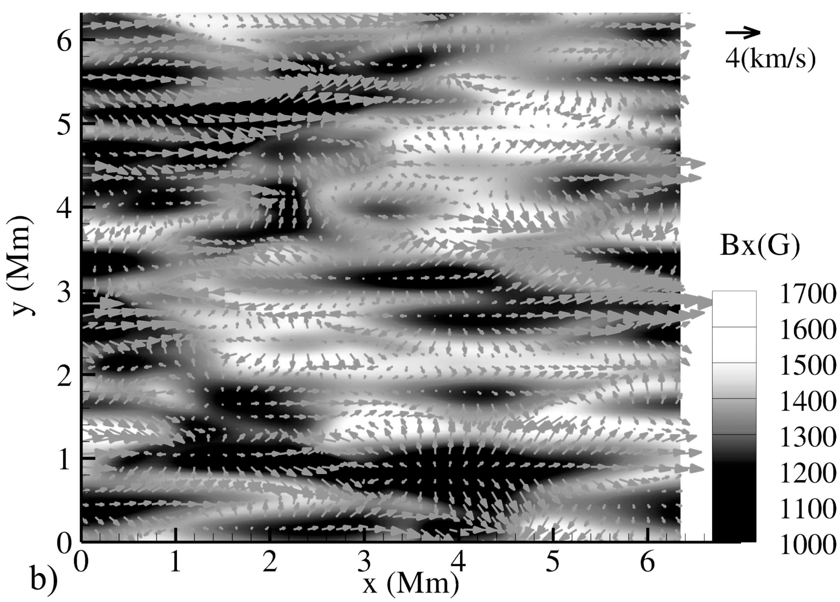

FIGURE 2. The gray-scale maps show snapshots of the magnetic field component, B_x, in the direction of the field inclination, and arrows show the horizontal velocity at the solar surface for different initial magnetic field strength: a) $B_0 = 1000$G, b) $B_0 = 1200$G. The inclination angle is $\alpha = 85^\circ$.

traveling convection waves, which become more apparent and stronger for higher field strengths and inclination. This convection develops long narrow structures of velocity, thermodynamic parameters and magnetic field, resembling the filamentary structure and motions in the penumbra of sunspots. These structures are illustrated in Figs 1 and 2.

Figure 1 shows a three-dimansional slice of our computational domain with a sample

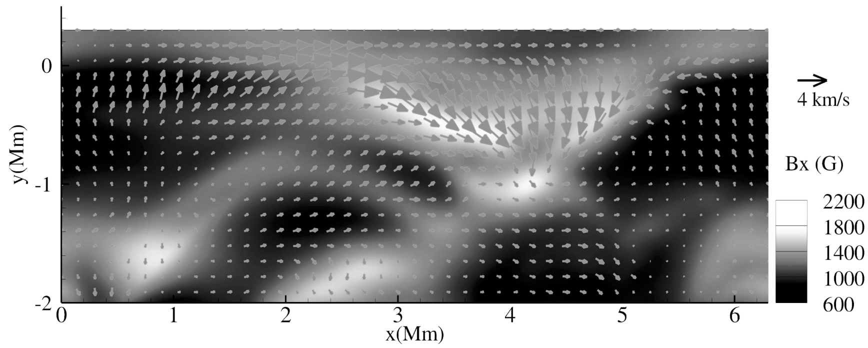

FIGURE 3. The same as Fig. 2 but a vertical xz-plane cut for $B_0 = 1000$ G and $\alpha = 85°$.

of magnetic field lines (grey curves), velocity field (black arrows), and a volume rendering of the temperature structures. The initial 1000 Gauss magnetic field is oriented in the xz-plane and inclined by 85 degrees to the z-axis, so that the B-vector is the positive in the x-direction. Evidently the strongest motions occur in the direction of the field inclination in narrow structures, with upflows and downflows at the initial and end points of these structures. The magnetic field lines change in accord with these elongated motions, rising up at the initial points and declining at the end points, thus giving an impression of rising and falling loop-like motions. The temperature is typically higher at the start points and lower at the end points. The typical vertical velocity around these points is about 1 km/s, but the horizontal velocity between them in the positive x-direction reaches $4 - 6$ km/s. Most of the horizontal mass flow occur in these relatively narrow patches, which strongly resemble Evershed clouds, discovered in observations (Shine *et al.* 1994). Significantly weaker flows in the opposite direction are also observed. These are often originate at the initial upflow points. Vertical cuts through the flow field (e.g., left yz-plane in Fig. 1) reveal associated vortex-type motions below the surface.

When the background field is strong, the horizontal flow patches become quite narrow, with the width of 0.5 Mm or less. The magnetic field variations also becomes more filamentary. This is illustrated in Fig. 2, which shows the surface structure of the horizontal flows and the B_x component for two different initial magnetic field strengths, 1000 and 1200 G. The simulations show strong interaction between the plasma flows and magnetic field. The magnetic field controls the general direction of the flows, but in the strong flow patches, the magnetic field is pushed aside and has a reduced magnetic field strength. This may give an impression, sometimes, reported from observations that the flows occur in magnetic field "gaps". Nevertheless, the plasma flows remain magnetized. The filamentary magnetic structures and flows are strongly coupled.

The most interesting feature of the simulations, which, we argue, is a key for understanding the Evershed effect, is the traveling wave pattern of magnetoconvection in the presence of a strongly inclined magnetic field. The simulations show that the velocity patches and magnetic field perturbations migrate in the direction of the field inclination. Vertical cuts in xz-planes show rapidly moving inclined convective cells (a snapshot is illustrated in Fig. 3). This process is best seen in the movies*, and also in the time-distance slices of the surface V_x velocity component along the x-axis. Fig. 4 shows an example of these slices for the initial magnetic field, $B_0 = 1200$ G, and the inclination

*http://soi.stanford.edu/∼irina/ApJL/movies.html

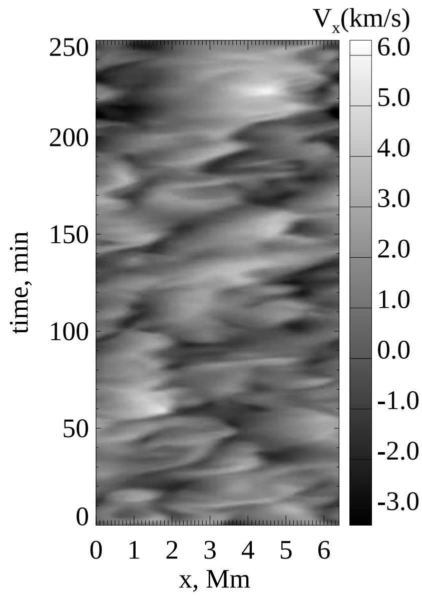

FIGURE 4. Time-space slice of the velocity component, V_x, in the direction of the field inclination for $B_0 = 1200$ G, $\alpha = 85°$.

angle of 85°. In this case the convective velocity reaches $\sim$ 6 km/s, and a pattern of convection waves traveling in the direction of the field inclination with a speed of 1 – 2 km/s can be identified.

The general picture is that the overturning convection motions are swept along by the traveling waves. This interaction amplifies the flows in the direction of the waves. This is accompanied by weaker plasma motions in the opposite direction. In fact, the initial points of the convective upflows often move in the opposite direction. This may explain the puzzling discrepancy between the outward flow direction and the apparent motion of "penumbra grains".

It is intriguing that the traveling convection pattern shows variations with a characteristic time of 20 – 50 min, resembling the quasi-periodic behavior noticed in the observations (Shine *et al.* 1994; Rimmele 1994; Georgakilas & Christopoulou 2003). By increasing the computational domain up to 25 Mm we have checked that the quasi-periodicity does not depend on the size of the domain and, thus, is not due to the periodic boundary condition. This is an intrinsic property of the inclined field magnetoconvection, but understanding of this phenomenon require further investigation.

As we have pointed out the high-speed (4 – 6 km/s) horizontal flows occur in localized patches corresponding to the Evershed clouds. An averaged over time and space velocity is smaller, about 1 – 2 km/s. The flows are concentrated in a shallow subsurface layer less than 1 Mm deep (Fig. 5, left panel). The velocity peaks about 100 – 200 km below the surface. This also corresponds to the observations showing that the velocity of the Evershed flows increases with depth. The averaged velocity does not change much with the magnetic field strength in the range of 1000 – 1500 G, but it strongly depends on the inclination angle (Fig. 5, right panel). The mean horizontal flow is much weaker for small inclination angles.

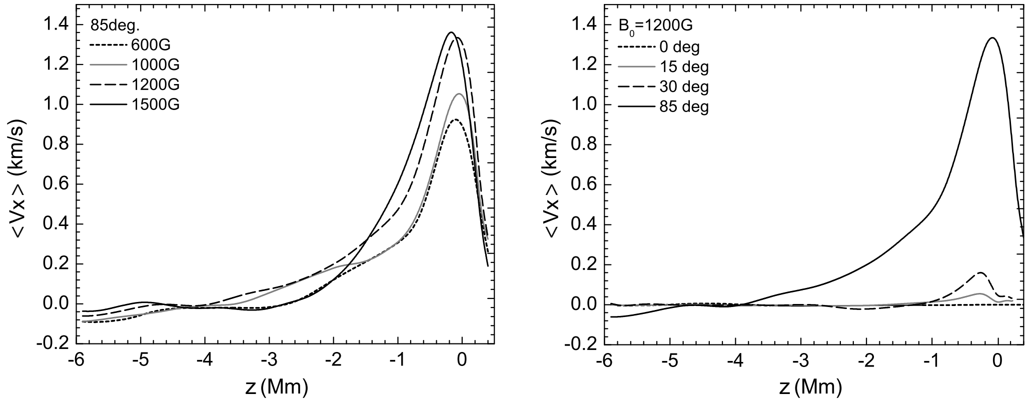

FIGURE 5. The distributions of the subsurface horizontal velocity component, V_x, with depth, z: for the magnetic field strength of 600, 1000, 1200, and 1500 G and the inclination angle, $\alpha = 85^\circ$ (left panel); $B_0 = 1200$ G, α=0, 15, 30 and 85 degrees (right panel).

4. Discussion

The radiative LES MHD simulations of solar magnetoconvection in regions of inclined magnetic field qualitatively and quantitatively describe many observed features of the Evershed effect in sunspots. The results indicate that the principal physical mechanism of the Evershed flows is the traveling wave nature of the magnetoconvection. The traveling waves have been extensively studied in idealized situations (Weiss 1991; Hurlburt *et al.* 1996), and it has been suggested that they play a significant role in sunspot flows (Hurlburt *et al.* 2000). Our simulations model this phenomenon in realistic solar conditions and show that, indeed, many details correspond to the observations, thus providing a basis for explaining the Evershed effect.

In particular, the simulations show that the high-speed flows reaching 4 – 6 km/s occur in the direction of the field inclination in narrow, 2 – 3 Mm long patches, which tend to appear quasi-periodically on the time-scale of 15 – 40 min. These patches correspond to the so-called Evershed clouds (Shine *et al.* 1994; Rimmele 1994; Cabrera Solana *et al.* 2007) and represent the main component of the Evershed flows. These horizontal flows originate from convective upflows of hotter plasma, similar to ordinary convection, but are channeled by the magnetic field and amplified by the traveling convective waves. The whole process is highly non-linear and stochastic with high-speed patches appearing randomly, but the simulations also show large-scale organization patterns across the simulation domain, which seem to be associated with the traveling waves. These patterns are evident in the simulation movies. Some observations showed a signature of coherence in appearance of the Evershed clouds (Shine *et al.* 1994), but this has not been fully established (Georgakilas & Christopoulou 2003). The simulations suggest that a large-scale coherence may be a fundamental property of the traveling wave phenomenon, and certainly encourage further observational studies. Of course, in real sunspots the magnetic field stricture is highly inhomogeneous, and this may affect the large-scale appearance. This must be investigated in future simulations.

In the past several models were suggested to explain the Evershed effect. Interestingly, some features of these models can be found in our simulations. One of the first models describes the penumbra filaments as convective rolls along the direction of magnetic field (Danielson 1961), which suggests the convective nature of the Evershed effect. A weakly

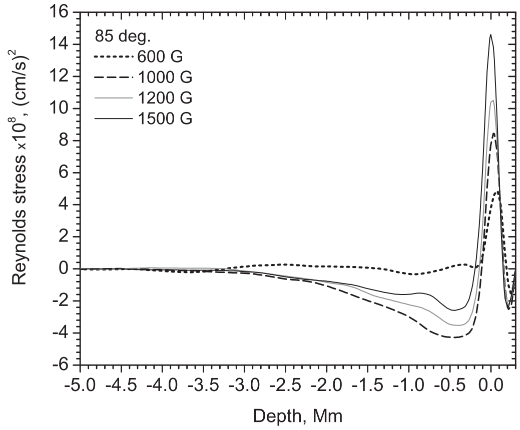

FIGURE 6. Reynolds stress profiles for different magnetic field strength of 600, 1000, 1200, and 1500 G, and the inclination angle, $\alpha = 85°$.

non-linear theory of convective rolls in inclined magnetic field showed that they generate a mean shear flow because of non-zero mean Reynolds stress (Busse 1987).

The apparent observed wave-like behavior inspired attempts to explain the Evershed effect as magnetoacoustic or magnetogravity waves (Maltby & Eriksen 1967; Bunte *et al.* 1993). Our model specifies that these waves are convective in nature. The rising and falling thin-flux tube model (Schlichenmaier *et al.* 1998) was suggested to describe the discrepancy between the apparent motion of penumbra features and the main Evershed flows. Our simulations have explained this and also revealed upward and downward loop-like motions of magnetic field lines synchronized with the high-velocity patches. The siphon model (Meyer & Schmidt 1968; Montesinos & Thomas 1997) suggested that the flow is driven by the pressure difference between the initial and end points, and indeed, in the simulations the gas pressure in the initial points is higher than at the end points. The recent numerical simulations of the sunspot structure (Heinemann *et al.* 2007; Rempel *et al.* 2009) have led to the suggestion that the Evershed effect is caused by the overturning convection (Scharmer *et al.* 2008), but the flow speed was not sufficiently high. Our simulations have shown that the high-speed matching the observations is achieved if the magnetic field is strong, 1000 – 1500 G, and highly inclined, when the magnetoconvection has properties of traveling waves. Thus, it seems that the MHD simulations provide a unified description of the models and the key observed features. Perhaps, this will lead to the understanding of the 100-year old discovery.

5. Future work

For further development we plan continuing investigation of convective motion in strong inclined magnetic field with increasing spatial resolution and will also investigate the mechanism of the mean shear flow in the presence of the inclined magnetic field. In particular, we plan to investigate the mechanism suggested by Busse (1987) that the Evershed shear flow is driven the correlated Reynolds stresses of convective rolls. Our preliminary results (Fig. 6) show that the mean Reynolds stress $< V_x V_z >$ has a positive gradient in a narrow subsurface layer, and thus can generate a shear flow. Alternative explanations may include generation of the shear flow by magnetic stress. The future work also includes the modeling of the whole sunspot structure and investigation of generation of acoustic waves by magnetic turbulence.

REFERENCES

Bunte, M., Darconza, G., & Solanki, S. K. 1993 Surface waves as the origin of the Evershed phenomenon. *Astron. & Astrophys.* **274**, 478–486.

Busse, F.H. 1987 A new mechanism for the Evershed flow. *Proc. of the Inaugural workshop and round table discussion for the D-E-S Telescope installations on the Canary Islands*, 187–196.

Cabrera Solana, D., Bellot Rubio, L. R., Beck, C., & Del Toro Iniesta, J. C. 2007 Temporal evolution of the Evershed flow in sunspots. I. Observational characterization of Evershed clouds. *Astron. & Astrophys.* **475**, 1067–1079.

Cabrera Solana, D., Bellot Rubio, L. R., Borrero, J. M., & Del Toro Iniesta, J. C. 2008 Temporal evolution of the Evershed flow in sunspots. II. Physical properties and nature of Evershed clouds. *Astron. & Astrophys.* **477**, 273–283.

Danielson, R. E. 1961 The structure of sunspot penumbras. II. Theoretical. *Astrophysical Journal* **134**, 289–311.

Evershed, J. 1909 Radial movement in sun-spots. *Mon. Not. R. Astr. Soc* **69**, 454–457.

Georgakilas, A. A., & Christopoulou, E. B. 2003 Temporal behavior of the Evershed effect. *Astrophysical Journal* **584**, 509–523.

Germano, M., Piomelli, U., Moin, P., & Cabot, W. H., & Del Toro Iniesta, J. C. 1991 A dynamic subgrid-scale eddy viscosity model. *Physics of Fluids* **3**, 1760–1765.

Heinemann, T., Nordlund, Å., Scharmer, G. B., & Spruit, H. C. 2007 MHD simulations of penumbra fine structure. *Astrophysical Journal* **669**, 1390–1394.

Hurlburt, N. E., Matthews, P. C., & Proctor, M. R. E. 1996 Nonlinear compressible convection in oblique magnetic fields. *Astrophysical Journal* **457**, 933–938.

Hurlburt, N. E.,Matthews, P. C., & Rucklidge, A. M. 2000 Solar magnetoconvection. *Solar Physics* **192**, 109–118.

Ichimoto, K., Suematsu, Y., Tsuneta, S., Katsukawa, Y., Shimizu, T., Shine, R. A., Tarbell, T. D., Title, A. M., Lites, B. W., Kubo, M., & Nagata, S. 2007a Twisting motions of sunspot penumbral filaments. *Science* **318**, 1597–1599.

Ichimoto, K., Shine, R. A., Lites, B., Kubo, M., Shimizu, T., Suematsu, Y., Tsuneta, S., Katsukawa, Yu., Tarbell, Th. D., Title, A. M., Nagata, Sh., Yokoyama, T., & Shimojo, M. 2007b Fine-scale structures of the Evershed effect observed by the Solar Optical Telescope aboard Hinode. *Publ. Astron. Soc. Japan* **59**, S593–S599.

Jacoutot, L., Kosovichev, A. G., Wray, A., & Mansour, N. N. 2008a Realistic numerical simulations of solar convection and oscillations in magnetic regions. *Astrophysical Journal Letters* **684**, L51–L54.

Jacoutot, L., Kosovichev, A. G., Wray, A., & Mansour, N. N. 2008b Numerical simulation of excitation of solar oscillation modes for different turbulent models. *Astrophysical Journal* **682**, 1386–1391.

Kitiashvili, I. N., Kosovichev, A. G., Wray, A. A., & Mansour, N. N. 2009 Traveling waves of magnetoconvection and the origin of the Evershed effect in sunspots *Astrophys. Journal Letters* **700**, L178–L181.

Maltby, P., & Eriksen, G. 1967 The Evershed effect as a wave phenomenon. *Solar Physics* **2**, 249–257.

Meyer, F., & Schmidt, H. U. 1968 The Evershed effect as a wave phenomenon. *Mitteilungen der Astronomischen Gesellschaft Hamburg* **25**, 194–196.

Moin, P., Squires, K., Cabot, W. & Lee, S. 1991 A dynamic subgrid-scale model for compressible turbulence and scalar transport. *Phys. Fluids A* **3**, 2746–2757.

Montesinos, B., & Thomas, J. H. 1997 The Evershed effect in sunspots as a siphon flow along a magnetic flux tube. *Nature* **3**, 485–487.

Rempel, M., Schüssler, M., & Knölker, M. 2009 Radiative magnetohydrodynamic simulation of sunspot structure *Astrophysical Journal* **691**, 640–649.

Rimmele, T. R. 1994 On the temporal behaviour of the Evershed effect. *Astronomy and Astrophysicsl* **290**, 972–982.

Rimmele, T. R. 1995 Evidence for thin elevated evershed channels. *Astronomy and Astrophysicsl* **298**, 260–276.

Rogers, F. J., Swenson, F. J & Iglesias, C. A. 1996 OPAL Equation-of-State tables for astrophysical applications *Astrophysical Journal* **456**, 902–908.

Scharmer, G. B., Nordlund, Å., & Heinemann, T. 2008 Convection and the origin of Evershed flows in sunspot penumbrae. *Astrophysical Journal Letters* **677**, L149–L152.

Schlichenmaier, R., Jahn, K., & Schmidt, H. U. 1998 A dynamical model for the penumbral fine structure and the Evershed effect in sunspots *Astrophysical Journal Letters* **493**, L121–L124.

Shine, R. A., Title, A. M., Tarbell, T. D., Smith, K., Frank, Z. A., & Scharmer, G. 1994 High-resolution observations of the Evershed effect in sunspots. *Astrophysical Journal* **430**, 413–424.

Smagorinsky, J. 1963 General circulation experiments with the primitive equations I. The basic experiment. *Monthly Weather Review* **93**(1), 99–164.

Stein, R. F., & Nordlund, Å 2002 Solar surface magneto-convection and dynamo action. *SOLMAG 2002. Proc. of the Magnetic Coupling of the Solar Atmosphere Euroconference* **505**, 83–89.

Theobald, M. L., Fox, P. A., & Sofia, S. 1994 A subgrid-scale resistivity for magnetohydrodynamics. *Phys. Plasmas* **1**(9), 3016–3032.

Tritschler, A. 2009 Structure and dynamics of sunspots. *ArXiv e-prints arXiv:0903.1300*, pp. 12.

Walker, M. R., & Barenghi, C. F. 1999 Nonlinear magnetoconvection and the geostrophic flow. *Physics of the Earth and Planetary Interiors* **111**, 35–46.

Weiss, N. O. 1991 Magnetoconvection. *Geophysical and Astrophysical Fluid Dynamics* **62**, 229–247.

Zhang, K. 1999 Nonlinear magnetohydrodynamic convective flows in the Earth's fluid core. *Physics of the Earth and Planetary Interiors* **111**, 93–103.